ARTICLE
Journal of Cellular Biochemistry 113:93–99 (2012)

Journal of Cellular Biochemistry

Oophorectomy-Induced Bone Loss is Attenuated in MAGP1-Deficient Mice

Clarissa S. Craft,[1] Thomas J. Broekelmann,[1] Wei Zou,[2] Jean C. Chappel,[2] Steven L. Teitelbaum,[2] and Robert P. Mecham[1*]

[1]*Department of Cell Biology and Physiology, Washington University School of Medicine, St. Louis, Missouri 63110*

[2]*Department of Anatomic and Molecular Pathology, Washington University School of Medicine, St. Louis, Missouri 63110*

ABSTRACT

Microfibril-associated glycoprotein-1 (MAGP1), together with the fibrillins, are constitutive components of vertebrate microfibrils. Mice deficient in MAGP1 (murine MAGP1 knockout animals (*Mfap2*$^{-/-}$); MAGP1Δ) is appropriate develop progressive osteopenia and reduced whole bone strength, and have elevated numbers of osteoclasts lining the bone surface. Our previous studies suggested that the increased osteoclast population was associated with elevated levels of receptor activator of NF-κB ligand (RANKL), a positive regulator of osteoclast differentiation. To explore the relationship between RANKL expression and osteoclast differentiation in MAGP1 deficiency, oophorectomy (OVX) was used to stimulate RANKL expression in both WT and MAGP1Δ animals. Bone loss following OVX was monitored using whole body DEXA and in vivo μCT. While WT mice exhibited significant bone loss following OVX, percent bone loss was reduced in MAGP1Δ mice. Further, serum RANKL levels rose significantly in OVX WT mice, whereas, there was only a modest increase in RANKL following OVX in the mutant mice due to already high baseline levels. Elevated RANKL expression was normalized when cultured MAGP1Δ osteoblasts were treated with a neutralizing antibody targeting free TGFβ. These studies provide support for increased RANKL expression associated with MAGP1 deficiency and provide a link to altered TGF-β signaling as a possible causative signaling pathway regulating RANKL expression in MAGP1Δ osteoblasts. J. Cell. Biochem. 113: 93–99, 2012.

KEY WORDS: MAGP1; MICROFIBRIL; BONE; OOPHORECTOMY; RANKL

Microfibrils are extracellular matrix (ECM) structures that impart strength to tissue, and regulate growth factor signaling by sequestering ligands within the matrix. The constitutive components of these fibers in vertebrates are the fibrillins (FBN-1,-2,-3) and MAGPs (MAGP-1,-2), [Cleary and Gibson, 1983; Sakai et al., 1986]. Importantly, microfibrils are known to interact with numerous other proteins, including ligands of the transforming growth factor-beta (TGFβ) superfamily [Dallas et al., 2000; Gregory et al., 2005]. Microfibrils are abundantly expressed in bone, and can be found in the periosteal matrix, surrounding osteocytes, chondrocytes, and osteons, on the endochondral surface, and within the trabecular matrix [Arteage-Solis and Ramirez, 2008]. Disruption of the fibrillins and microfibril-associated glycoprotein-1 (MAGP1) induces an array of phenotypes that can affect both the appendicular and axial skeleton [Ramirez et al., 2008; Weinbaum et al., 2008; Craft et al., 2010]. A phenotype common to fibrillin and MAGP1 mutation/deletions is diminished bone mass. However, the mechanisms whereby microfibrils regulate bone remodeling have been largely unappreciated.

Bone remodeling, the balance of bone resorption, and new bone formation, is necessary for maintaining bone quality. This process is coordinated by the coupling of osteoclasts (resorption) and osteoblasts (formation). Bone loss associated with post-menopausal osteoporosis, rheumatoid arthritis, and lytic bone metastases are typically the consequence of excess osteoclast activation, and thus increased bone resorption [Rodan and Martin, 2000; Takayanagi

Abbreviations: MAGP1, microfibril-associated glycoprotein-1; MAGP1Δ, murine MAGP1 knockout animals (*Mfap2*$^{-/-}$); TGFβ, transforming growth factor-beta; BMP, bone morphogenetic protein; Tb, trabecular bone; BMD, bone mineral density; RANKL, receptor activator of NF-κB ligand.

Grant sponsor: NIH; Grant numbers: HL71960, HL084922, T32-HL007275-30, AR0327888, AR046523, AR057037, AR054618; Grant sponsor: National Marfan Foundation Research Grant; Grant sponsor: Washington University Core Center for Musculoskeletal Biology and Medicine; Grant sponsor: NIH; Grant number: P30AR057235.

*Correspondence to: Dr. Robert P. Mecham, Department of Cell Biology and Physiology, Washington University School of Medicine, Campus Box 8228, 660 S. Euclid Ave., St. Louis, MO 63110. E-mail: bmecham@wustl.edu

Received 11 August 2011; Accepted 17 August 2011 • DOI 10.1002/jcb.23331 • © 2011 Wiley Periodicals, Inc.
Published online 24 August 2011 in Wiley Online Library (wileyonlinelibrary.com).

et al., 2000; Katagiri and Takahashi, 2002]. The receptor activator of NF-κB (RANK) signaling pathway is necessary for osteoclastogenesis [Boyce and Xing, 2007]. Osteoblasts stimulate osteoclastogenesis through RANK ligand (RANKL) expression, and block it by osteoprotegerin production (OPG, the decoy RANKL receptor). Because of their regulatory roles, the RANKL:OPG ratio is considered an important predictor of skeletal dynamics [Hofbauer and Schoppet, 2004].

We recently reported that MAGP1 deficient (murine MAGP1 knockout animals (*Mfap2*$^{-/-}$); MAGP1Δ) mice develop progressive bone loss and have reduced whole bone strength [Craft et al., 2010]. Utilizing in vitro and in vivo assays, we found no significant difference in MAGP1Δ osteoblast differentiation or function (mineralization capacity). However, significantly more osteoclasts are found in MAGP1Δ bone. This difference is due to MAGP1Δ bone marrow macrophages (BMM) being sensitized to RANKL as demonstrated by more MAGP1Δ BMMs differentiating to osteoclasts than do WT cells when exposed to a similar amount of RANKL. Nistala et al. [Nistala et al., 2010a,b] subsequently demonstrated enhanced osteoclastogenesis in fibrillin-deficient mice. Together, these studies show that osteoblasts derived from mice deficient in MAGP1, FBN1, or FBN2 all express higher levels of RANKL Craft et al., 2010; Nistala et al., 2010a,b] and establish that microfibrils are important regulators of RANKL-RANK signaling and thus bone homeostasis.

RANKL expression is elevated in women with post-menopausal osteoporosis, as well as in oophorectomized rodents [Eghbali-Fatourechi et al., 2003; Ominsky et al., 2008]. Further, RANKL inhibition blunts oophorectomy (OVX)-induced bone loss [Samadfam et al., 2007; Ominsky et al., 2008]. If increased expression or sensitivity to RANKL is a cause for the low bone mass of MAGP1Δ mice [Craft et al., 2010], then it is possible that MAGP1Δ mice will have an attenuated response to OVX because of an inability to raise RANKL expression above their already high levels. Here we show that the increase in RANKL expression in MAGP1Δ mice following OVX is less than that seen in oophorectomized WT mice and that the mutant mice lose less bone following OVX, relative to WT mice. We also establish a link between elevated RANKL expression and TGF-β signaling in MAGP1 deficiency.

MATERIALS AND METHODS

NOMENCLATURE

The gene name for MAGP1 is *Mfap2*, whereas, the gene name for MAGP2 is *Mfap5*. To avoid confusing MAGP1 and MAGP2 when referring to knockout mice, we will refer to the MAGP1 knockout genotype (*Mfap2*$^{-/-}$) as MAGP1Δ.

MATERIALS

Recombinant human TGFβ1 was acquired from R&D Systems (Minneapolis, MN), and used at a final concentration of 2 ng/ml in signaling assays and 200 ng/ml for surface plasmon resonance. Recombinant mouse TNFα was acquired from R&D Systems, and used at a final concentration 1 μg/ml for surface plasmon resonance. Recombinant glutathione *S*-transferase (GST)-RANKL was expressed/purified as described [Lam et al., 2000], and used at a final concentration of 10 μg/ml. Neutralizing TGFβ (-1,-2,-3) and TNFα antibodies were acquired from R&D Systems and used at a final concentration of 300 ng/ml.

STATISTICAL ANALYSIS

Paired *t*-test was used to determine statistical significance between genotypes. Values were considered significantly different when *P*-values were <0.05. Sample sizes are provided in figure legends.

ANIMALS

Generation and genotyping of the MAGP1Δ colony has been described [Weinbaum et al., 2008]. Oophorectomies were performed on 3- to 4-month-old female mice. Calvaria osteoblasts were harvested from 3 to 5 days old mice. All mice were in the Black Swiss background (BkSw, Taconic; Hudson, NY) and were housed in a pathogen-free animal facility, fed standard chow ad libitum, and treated following animal protocols approved by the Washington University Animal Studies Committee.

ANIMAL PROCEDURES

Oophorectomy. OVX or sham surgeries were performed as described in [Lai et al., 2006] with the following modifications. Mice were anesthetized using 2% isoflurane, ovaries were exposed through an abdominal approach, and removed by cauterization. The peritoneum and skin were sutured separately. Pain was managed by subcutaneous injection of 0.075 mg/kg bupernorphine (2/day for 3 days) followed acetaminophen diluted in the drinking water (32 mg/ml) for 1 week.

Radioimaging—DEXA and in vivo μCT. Detailed procedures can be found elsewhere [Craft et al., 2010]. Briefly, whole body composition measurements, excluding the head, were made by dual energy X-ray absorptiometry (DEXA; PIXImus Lunar-GE). Trabecular bone mineral density (BMD) and bone volume (BV/TV) were determined using in vivo μCT (VivaCT 40, Scanco Medical). Baseline scans were performed prior to surgery then at 2–4 weeks intervals post-OVX. Both scanning modalities were calibrated at regular intervals, and one person was responsible for all scanning.

Serum collection. For serum collection, mice were fasted (food and water) for 12 h. Blood was collected by submandibular bleed or cardiac puncture. Serum was separated using BD brand microtainer-SST tubes, aliquoted, and stored at −80°C.

SERUM RANKL QUANTIFICATION

Serum RANKL was determined using the commercially available mouse RANKL quantikine kit from R&D Systems, following the manufacturer's protocol.

SURFACE PLASMON RESONANCE ASSAYS

Interactions between proteins were studied by surface plasmon resonance using the BIAcore X system (Uppsala, Sweden) as previously described [Werneck et al., 2008], but with the following modifications. Recombinant mouse MAGP1 (3000RU) was covalently immobilized on the BIAcore CM-5 sensor chip (carboxylated dextran matrix) according to the manufacturer's instructions. Analytes were prepared in HBST buffer (25 mM HEPES, 150 mM

NaCl, and 0.01% Tween20) at the following concentrations: TGFβ-1 (0.2 μg/ml), TNFα (1 μg/ml), and RANKL (10 μg/ml). Analytes were injected at a flow rate of 40 μl/min.

STABLE EXPRESSION OF MAGP1 IN RFL-6 CELLS

Rat lung fibroblast (RFL-6) cells were acquired from the ATCC and grown in HAM's F-12 media (20% FBS). These cells assemble microfibrils in culture, but are naturally devoid of MAGP1. Consequently, full length MAGP1 (or vector control construct) was introduced to these cells by stable transfection and G418 selection. Constructs and methods for stable transfection have been described [Segade et al., 2007].

PRIMARY CELL ISOLATION AND CULTURE

Wild-type and MAGP1Δ calvaria osteoblasts were isolated from 3 to 5 days old littermates. Calvaria isolation was as previously described [Craft et al., 2010]. Osteoblasts were allowed to expand for 3–4 days, trypsinized, and seeded at a density of 1×10^4 cells/cm^2. For inhibitor studies, 1 day after plating, media was supplemented with neutralizing TGFβ-1/2/3 antibody (300 ng/ml, R&D), neutralizing TNFα antibody (300 ng/ml, R&D), or PBS for 4 days.

IMMUNOFLUORESCENCE

MAGP1 incorporation into the ECM of cultured RFL-6 cells was detected via immunofluorescence. Cells were cultured for 7 days post-confluence in plastic Lab-Tek chamber slides. Cells were fixed in methanol, blocked with PBS containing 5% normal goat serum, incubated with rabbit anti-MAGP1 primary antibody overnight, and detected with Alexa Fluor® 555 secondary antibody. Cover slips were applied using Permount mounting media with DAPI.

RNA AND PROTEIN ANALYSES

RNA purification, reverse transcription, and quantification of RANKL (via qPCR) were performed as previously described [Craft et al., 2010]. For protein studies, RFL-6 cells were grown for 7 days post-confluence then serum starved for 24 h. Cell lysis, electrophoresis, and immunoblotting were performed as previously described [Craft et al., 2010] with the exception that immunoblotting utilized phosphorylation-specific Smad2 (p-smad2), and total-protein smad2 (t-smad2) antibodies (both from Cell Signaling Technology).

RESULTS

CHARACTERIZATION OF FEMALE MAGP1Δ MICE

We previously reported that MAGP1 deficiency in male mice diminishes bone mass. Using whole body DEXA scan to compare body composition, in this study we found similar traits in female MAGP1Δ mice. Compared to WT animals, 3-month-old female MAGP1Δ mice were slightly heavier (not statistically significantly) and had significantly less (−6%) whole body BMD (Table I).

TABLE I. Whole Body Composition Analysis (Baseline)

	BMD (g/cm^2)	% Fat	Body Weight (g)
WT	0.050 ± 0.001	20.7 ± 2.0	21.6 ± 1.5
−/−	0.047 ± 0.001*	22.6 ± 4.2	22.4 ± 1.8

Whole body DEXA scans were performed on 3-month-old female WT and MAGP1Δ mice. N = 12 and 10 for WT and MAGP1Δ mice, respectively. Data are presented as AVG ± SD, *$P < 0.05$.

MAGP1Δ MICE HAVE REDUCED BONE LOSS FOLLOWING OVX

Estrogen depletion, as a consequence of OVX, induces bone resorption by stimulating RANKL production. OVX or sham surgeries were performed on 3- to 4-month-old WT and MAGP1Δ females to induce bone loss. Whole body DEXA and in vivo μCT of tibial trabecular bone (Tb) were used to monitor relative bone loss in the mice. Table II provides whole body composition data obtained via DEXA scan on the sham and OVX operated mice 8 weeks after surgery. As expected, WT mice lost a significant proportion of their whole body BMD (−5.7%). However, there was no statistical difference in whole body BMD between sham and OVX-operated MAGP1Δ mice. Increased percent body fat (% fat) is associated with OVX, and was apparent in both genotypes. Estrogen depletion by OVX was confirmed by measuring uterine wet weights at the time of death (Table II). MAGP1 deficiency alone had no effect on uterine weight, whereas OVX significantly decreased uterine weight in both WT and MAGP1Δ mice (86% and 81%, respectively).

In vivo μCT provides precise measurements of volumetric BMD and bone volume (BV/TV). Figure 1 shows results from a longitudinal study following the changes in BMD and BV/TV from tibial Tb at 2, 4, and 8 weeks post-sham or OVX surgery. Using this modality it was even more evident that MAGP1Δ mice are less susceptible to OVX-induced bone loss than WT. As seen in Figure 1A, WT mice steadily lose trabecular BMD (tbBMD) following OVX, loosing an average of 45% of their tbBMD by 8 weeks. In contrast, despite an immediate reduction in tbBMD following OVX, MAGPΔ mice have little tbBMD loss 2 weeks following surgery. By 8 weeks, MAGP1Δ mice have lost only 26% of the trabecular BMD, relative to baseline tbBMD. Figure 1B demonstrates a similar trend for trabecular BV/TV (tbBV/TV) in the WT and MAGP1Δ following OVX or sham surgery. To confirm these findings, OVX surgeries were performed on a larger cohort of WT and MAGP1Δ mice (no sham surgeries were performed in this study). Similar to the first OVX study, both WT and MAGP1Δ mice lose a significant amount of trabecular BMD and BV/TV during the first 2 weeks following surgery (Fig. 2). However, unlike the WT mice, which continue to loose significant amounts of both tbBMD and tbBV/TV between 2 and 12 weeks post-surgery, there is no significant change in MAGP1Δ mice over this time period.

TABLE II. Whole Body Composition Analysis (8 Weeks Post-OVX)

	BMD (g/cm^2)	% Fat	Body Weight (g)	Uterine Weight (g)
WT Sham	0.053 ± 0.001	18.5 ± 2.6	22.8 ± 2.1	0.101 ± 0.002
WT OVX	0.050 ± 0.001*	28.8 ± 3.0*	27.5 ± 2.4*	0.014 ± 0.033*
−/− Sham	0.051 ± 0.001	21.7 ± 2.9	24.7 ± 2.2	0.088 ± 0.002
−/− OVX	0.049 ± 0.001	29.1 ± 2.3*	27.6 ± 1.1*	0.017 ± 0.015*

Whole body DEXA scans were performed on OVX or sham-operated animals 8 weeks post-surgery. Uterine weights were obtained on the following days. N = 3 (WT-sham), 7 (WT-OVX), 4 (MAGP1Δ-sham), and 3 (MAGP1Δ-OVX). Data are presented as AVG ± SD, *$P < 0.05$.

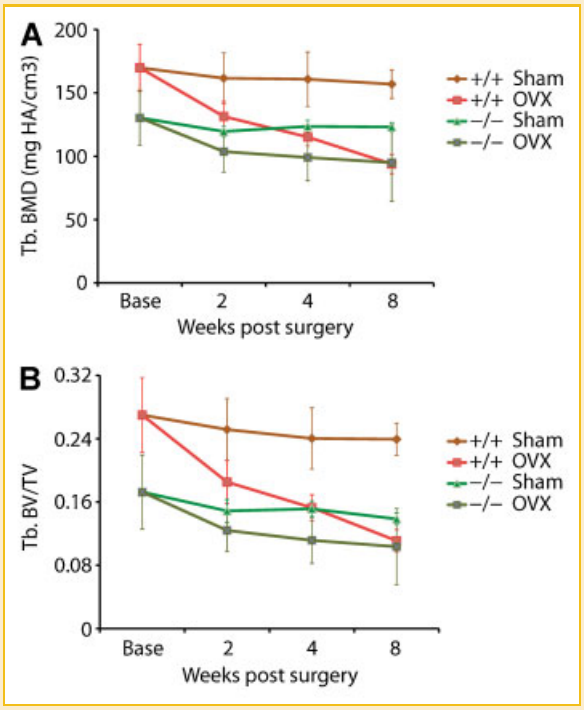

Fig. 1. MAGP1Δ mice show a blunted response to OVX-induced bone loss. Trabecular BMD (A) and BV/TV (B) pre- and post-surgery were determined by in vivo μCT. N = 4 (WT-sham), 6 (WT-OVX), 4 (MAGP1Δ-sham), and 3 (MAGP1Δ-OVX). Data are presented as AVG ± SD, $^{*}P < 0.05$.

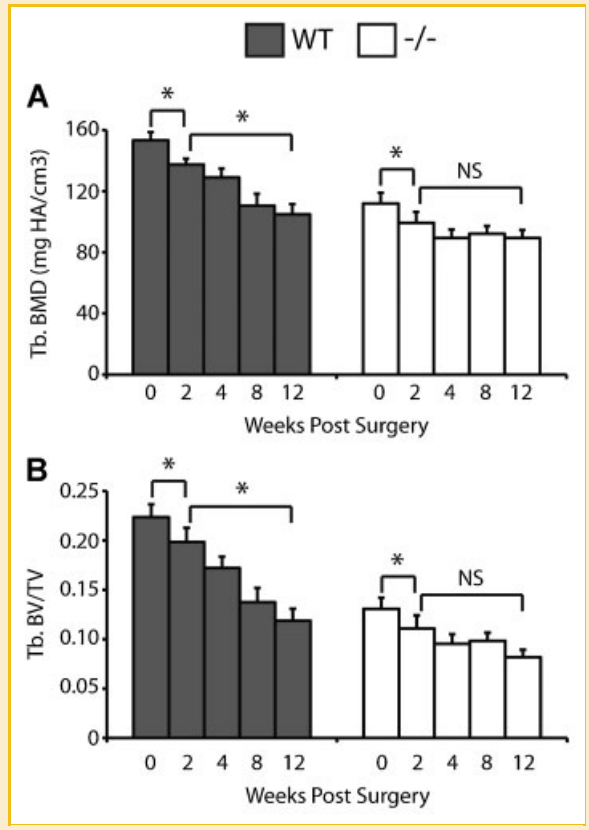

Fig. 2. OVX-induced bone loss stabilizes in MAGP1Δ mice by 2 weeks post-OVX. Trabecular BMD (A) and BV/TV (B) pre- and post-surgery were determined by in vivo μCT. N = 7 (WT-OVX) and 6 (MAGP1Δ-OVX). Data are presented as AVG ± SD, $^{*}P < 0.05$, NS, not significantly different.

OVX-INDUCED RANKL PRODUCTION IS BLUNTED IN MAGP1Δ MICE

MAGP1 deficiency results in an increase in RANKL production with no effect on OPG levels [Craft et al., 2010]. Consequently, the ratio of RANKL to OPG is skewed in favor of osteoclastogenesis in MAGP1Δ cells and mice. To investigate the relationship between RANKL levels and the change in BMD that occurs following OVX, RANKL levels were quantified in serum of WT and MAGP1Δ animals. As predicted, WT mice responded to OVX with a robust increase in RANKL serum concentration (2.2 fold) (Fig. 3). As was found in our previous study [Craft et al., 2010], basal RANKL levels were elevated in sham operated MAGP1Δ mice relative to WT controls, however, there was no significant difference in serum RANKL concentration between oophorectomized WT and MAPG1Δ mice. Consequently, the percent increase in serum RANKL following OVX was not as great in mutant mice as in the WT animals (48% vs. the 120% increase seen in WT mice). These studies suggest that MAGP1Δ mice are less responsive to OVX-induced bone loss and this phenotype is associated with their elevated basal RANKL production.

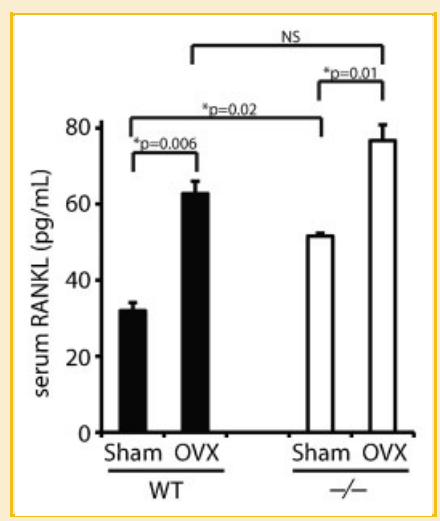

Fig. 3. Serum RANKL is elevated in MAGP1Δ mice. Serum was collected 6 weeks post-surgery. N = 6 (WT-sham), 7 (WT-OVX), 5 (MAGP1Δ-sham), and 8 (MAGP1Δ-OVX). Data are presented as AVG ± SE, $^{*}P < 0.05$.

MAGP1 INTERACTS SPECIFICALLY WITH TGFβ BUT NOT RANKL OR TNFα

The ECM functions as a reservoir for numerous growth factors that have the ability to regulate cell differentiation. Microfibrils, in particular, have a role in tissue homeostasis due to their ability to regulate the bioavailability of TGF-β [Neptune et al., 2003; Ramirez and Dietz, 2009]. We have reported that MAGP1 binds active TGF-β1 with high affinity [Weinbaum et al., 2008]. To investigate

whether MAGP1 regulates osteoclastogenesis by binding and sequestering the pro-osteoclastogenic factors RANKL and TNFα, surface plasmon resonance was used to study interactions between these proteins and recombinant MAGP1. MAGP1 was coated onto a CM-5 chip while recombinant TNFα, RANKL, and TGFβ-1 served as analytes. As seen in Figure 4A, MAGP1 has a strong affinity for TGFβ-1, whereas, binding was undetectable for either RANKL or TNFα.

To confirm that MAGP1 has a functional role in the regulation of TGFβ production, we evaluated MAGP1's ability to alter TGFβ-associated signaling in vitro. For these experiments we utilized the RLF-6 cell line that is naturally devoid of MAGP1 yet forms fibrillin-rich microfibrils (unpublished data). Stable transfections were performed with an expression vector encoding MAGP1 driven by a constitutive promoter or using an empty vector as a control (VC). Incorporation of plasmid-derived MAGP1 into the ECM was confirmed via immunofluorescence (Fig. 4B). To evaluate downstream TGFβ signaling (smad-2 phosphorylation, pSMAD2), cells were serum-starved after having been allowed to produce an ECM. Then pSMAD-2 was assessed in the presence or absence of exogenous TGFβ-1. As seen in Figure 4C, the presence of MAGP1 reduced basal TGFβ signaling and significantly blunted exogenous TGFβ-1-induced SMAD-2 phosphorylation.

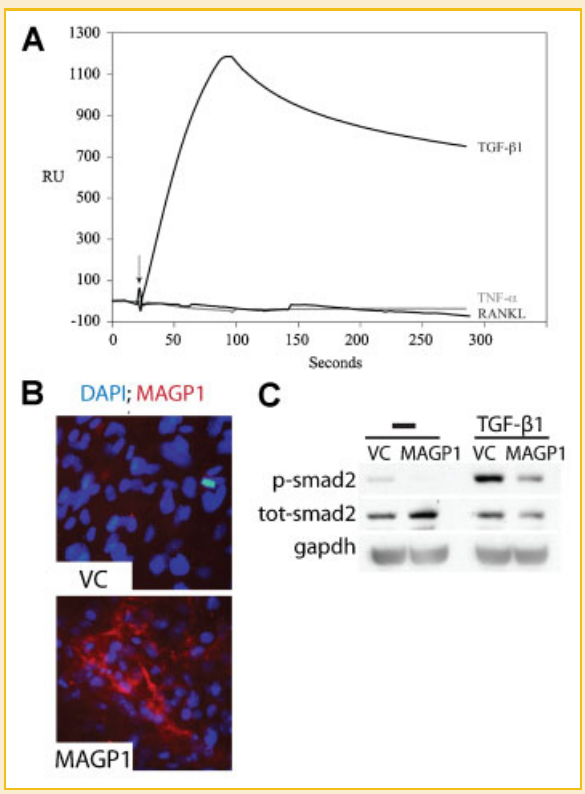

Fig. 4. MAGP1 binds TGFβ1 and regulates its bioavailability. (A) Surface plasmon resonance (BIAcore) was utilized to determine MAGP1's affinity for pro-osteoclastogenic factors TGFβ1, RANKL, and TNFα. (B,C) RFL-6 cells were stably transfected with full-length MAGP1 or control vector (VC). Cells were cultured for 7 days to allow development of ECM devoid (VC) or enriched with MAGP1. (C) Basal (unstimulated) or exogenous TGFβ1-induced SMAD-2 activation was determined by SDS–PAGE and immunoblotting with antibodies specific to phosphorylated SMAD-2 (p-smad2) or total smad-2 (tot-smad2).

DYSREGULATED TGFβ SIGNALING IN MAGP1-DEFICIENT OSTEOBLASTS ENHANCES RANKL PRODUCTION

To examine whether an increase in free TGFβ was responsible for the elevated RANKL expression seen in MAGP1Δ osteoblasts (Fig. 5), calvaria osteoblasts were cultured in the presence of a neutralizing antibody that reacts with TGFβ isoforms -1,-2,-3. A neutralizing antibody targeting TNFα served as a negative control, as MAGP1 does not bind this molecule (Fig. 4A). As expected, basal RANKL expression was elevated in MAGP1Δ cells. Importantly, neutralization of TGFβ abrogated this increase while neutralization of TNFα had no effect. These findings suggest that MAGP1-mediated regulation of TGFβ activity is upstream of RANKL expression.

DISCUSSION

MAGP1 is a component of vertebrate microfibrils where it interacts with fibrillin to influence microfibril function. Inactivation of the MAGP1 gene (*Mfap2*) in mice resulted in numerous phenotypes, including a bleeding abnormality, delayed dermal wound healing, increased adiposity, and the development of spontaneous bone fractures [Weinbaum et al., 2008; Werneck et al., 2008]. Detailed investigation of the skeletal phenotype found that MAGP1Δ mice undergo progressive bone loss that is associated with an increase in osteoclast number [Craft et al., 2010]. Characterization of osteoblasts in MAGP1Δ animals found normal numbers and normal function in terms of their ability to form bone. A major difference in MAGP1Δ osteoblasts versus WT, however, was increased production of RANKL. Because of the importance of RANKL in directing osteoclast differentiation, elevated RANKL expression in MAGP1Δ osteoblasts likely contributes to the change in osteoclast number.

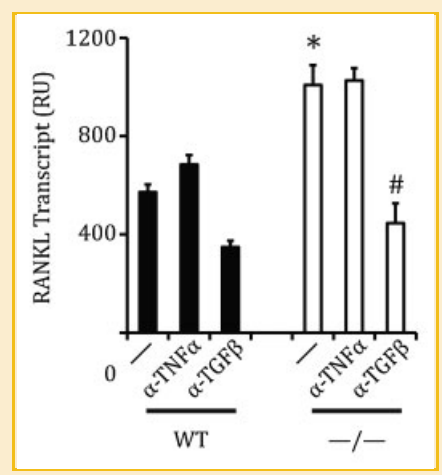

Fig. 5. Elevated RANKL expression is linked to increased free TGFβ. RANKL transcript was determined by RT-qPCR. Calvaria osteoblasts were cultured for 4 days in the presence of 300 ng/ml neutralizing antibodies targeting TGFβ(-1,-2,-3) or TNFα. N = 3 per group. Data are presented as RU (RANKL normalized to cyclophilin) AVG ± SD, $^{*}P < 0.05$.

In the results detailed in this report, we used OVX to investigate the significance of elevated RANKL production to the reduced bone mass phenotype seen in MAGP1Δ mice. Estrogen depletion, which occurs during menopause and following OVX, induces bone loss through the upregulation of RANKL [Eghbali-Fatourechi et al., 2003; Samadfam et al., 2007; Ominsky et al., 2008]. Our hypothesis was that because MAGP1 deficiency results in chronically elevated RANKL levels, MAGP1Δ mice might not be able to further increase RANKL production and, hence, would have attenuated OVX-induced bone loss. Indeed, MAGP1Δ mice exhibited only a modest loss in whole body BMD as well as trabecular BMD and BV/TV relative to WT mice. Serum measurements of RANKL confirmed a smaller percent increase in RANKL following OVX in MAGP1Δ mice compared to WT controls. These results show a relationship between modified RANKL levels and bone loss in MAGP1Δ mice.

The mechanism whereby MAGP1 influences RANKL expression is suggested by overlapping skeletal phenotypes associated with mutations in its microfibril binding partner, fibrillin. Individuals harboring fibrillin mutations display an array of abnormalities affecting the axial and appendicular skeleton [Ramirez et al., 2008]. Numerous studies have documented the ability of fibrillin to bind the TGF-β large latent complex and mice harboring fibrillin mutations show enhanced TGF-β signaling in affected tissues because TGF-β is no longer sequestered when microfibrils are disrupted. Like the MAGP1-deficient mouse, animals with fibrillin mutations share osteopenia and increased RANKL expression as a common skeletal phenotype [Pereira et al., 1999; Barisic-Dujmovic et al., 2007; Arteage-Solis and Ramirez, 2008; Nistala et al., 2010a,b,c]. A specific linkage between TGF-β and the skeletal phenotype in fibrillin-mutant mice was made by Nistala et al. [Nistala et al., 2010a,b,c] who showed that enhanced RANKL production and increased osteoclastogenesis associated with fibrillin mutations are downstream of improper TGFβ signaling. Our results demonstrate that elevated RANKL production, associated with MAGP1 depletion, is also downstream of an increase in free TGFβ, as addition of TGF-β specific neutralizing antibody to MAGP1Δ osteoblast cultures normalizes RANKL expression to that seen in WT osteoblasts. Further evidence supporting a relationship between microfibrils and TGF-β regulation are phenotypic similarities associated with fibrillin disruption and TGFβ receptors-I and -II mutation Loeys et al., 2005, 2006].

MAGP1's ability to bind active TGF-β raised the possibility that it might bind other factors known to regulate osteoclastogenesis. However, in surface plasmon surface resonance studies, MAGP1 did not bind RANKL itself nor did it interact with TNFα, a cytokine known to support osteoclastogenesis and stimulate RANKL expression. To confirm that MAGP1's interaction with TGFβ had functional significance, we used RFL-6 cells to evaluate the effect of MAGP1's presence (or absence) on downstream TGFβ-associated signaling (phosphorylation of smad2). These cells do not produce MAGP1 so the microfibrillar network they produce is mostly fibrillin. When MAGP1 was added to cultures of confluent cells, the ability of exogenous TGFβ-1 to stimulate smad-2 phosphorylation was blunted, suggesting MAGP1 functions as a sink for active TGFβ. Normalization of RANKL expression in MAGP1Δ osteoblasts to WT levels using a TGF-β-specific antibody lends further support to the sequestration role of MAGP1.

In summary, the similar skeletal phenotype in fibrillin and MAGP1 mutant mice suggests that both proteins contribute to a common mechanism of bone cell regulation. Like fibrillin, MAGP1 can interact with TGF-β (Fig. 4A) but differs from fibrillin in its capacity to bind the active form of the growth factor. MAGP1's binding site on fibrillin has been mapped to fibrillin's growth factor binding region and the presence of MAGP1 can interfere with fibrillin's interaction with latent TGF-β [Massam-Wu et al., 2010]. Since microfibrils contain both proteins, mutation of one will undoubtedly affect the biological properties of the other, which is an explanation for the overlapping phenotype when either protein is mutated. These results illustrate the complexity of microfibril biology and demonstrate that necessity of studying the role of microfibril-accessory proteins, in addition to fibrillin, in order to understand microfibril function.

ACKNOWLEDGMENTS

We thank Monica Croke for technical support, Christopher Ciliberto for animal colony maintenance, and Terese Hall for administrative support. We also thank Richard Pierce for his work in generating the MAGP1 knockout mouse. This work was supported by NIH grants HL71960, HL084922 (R.P. Mecham), T32-HL007275-30 (C.S. Craft), AR0327888, AR046523, AR057037, AR054618 (S.L. Teitelbaum), and a National Marfan Foundation Research Grant (R.P. Mecham). We also acknowledge the support from the Washington University Core Center for Musculoskeletal Biology and Medicine, NIH P30AR057235.

REFERENCES

Arteage-Solis E, Ramirez F. 2008. Marfan syndrome and related disorders of the connective tissue. In: Rosen CJ, editor. Primer on the metabolic bone diseases and disorders of mineral metabolism. Washington, DC: American Society for Bone and Mineral Research. pp 450–454.

Barisic-Dujmovic T, Boban I, Adams DJ, Clark SH. 2007. Marfan-like skeletal phenotype in the tight skin (Tsk) mouse. Calcif Tissue Int 81:305–315.

Boyce BF, Xing L. 2007. Biology of RANK, RANKL, and osteoprotegerin. Arthritis Res Ther 9 (Suppl 1): S1.

Cleary EG, Gibson MA. 1983. Elastin-associated microfibrils and microfibrillar proteins. Int Rev Connect Tissue Res 10:97–209.

Craft CS, Zou W, Watkins M, Grimston SK, Brodt MD, Broekelmann TJ, Weinbaum JS, Teitelbaum SL, Civitelli R, Silva MJ, Mecham RP. 2010. Microfibril-associated glycoprotein-1 (MAGP1), an extracellular matrix regulator of bone remodeling. J Biol Chem 283(37):25533–25543.

Dallas SL, Keene DR, Bruder SP, Saharinen J, Sakai LY, Mundy GR, Bonewald LF. 2000. Role of the latent transforming growth factor beta binding protein 1 in fibrillin-containing microfibrils in bone cells in vitro and in vivo. J Bone Miner Res 15:68–81.

Eghbali-Fatourechi G, Khosla S, Sanyal A, Boyle WJ, Lacey DL, Riggs BL. 2003. Role of RANK ligand in mediating increased bone resorption in early postmenopausal women. J Clin Invest 111:1221–1230.

Gregory KE, Ono RN, Charbonneau NL, Kuo CL, Keene DR, Bachinger HP, Sakai LY. 2005. The prodomain of BMP-7 targets the BMP-7 complex to the extracellular matrix. J Biol Chem 280:27970–27980.

Hofbauer LC, Schoppet M. 2004. Clinical implications of the osteoprotegerin/RANKL/RANK system for bone and vascular diseases. JAMA 292:490–495.

Katagiri T, Takahashi N. 2002. Regulatory mechanisms of osteoblast and osteoclast differentiation. Oral Dis 8:147–159.

Lai CF, Cheng SL, Mbalaviele G, Donsante C, Watkins M, Radice GL, Civitelli R. 2006. Accentuated ovariectomy-induced bone loss and altered osteogenesis in heterozygous N-cadherin null mice. J Bone Miner Res 21:1897–1906.

Lam J, Takeshita S, Barker JE, Kanagawa O, Ross FP, Teitelbaum SL. 2000. TNF-alpha induces osteoclastogenesis by direct stimulation of macrophages exposed to permissive levels of RANK ligand. J Clin Invest 106:1481–1488.

Loeys BL, Chen J, Neptune ER, Judge DP, Podowski M, Holm T, Meyers J, Leitch CC, Katsanis N, Sharifi N, Xu FL, Myers LA, Spevak PJ, Cameron DE, De Backer J, Hellemans J, Chen Y, Davis EC, Webb CL, Kress W, Coucke P, Rifkin DB, De Paepe AM, Dietz HC. 2005. A syndrome of altered cardiovascular, craniofacial, neurocognitive and skeletal development caused by mutations in TGFBR1 or TGFBR2. Nat Genet 37:275–281.

Loeys BL, Schwarze U, Holm T, Callewaert BL, Thomas GH, Pannu H, De Backer JF, Oswald GL, Symoens S, Manouvrier S, Roberts AE, Faravelli F, Greco MA, Pyeritz RE, Milewicz DM, Coucke PJ, Cameron DE, Braverman AC, Byers PH, De Paepe AM, Dietz HC. 2006. Aneurysm syndromes caused by mutations in the TGF-beta receptor. N Engl J Med 355:788–798.

Massam-Wu T, Chiu M, Choudhury R, Chaudhry SS, Baldwin AK, McGovern A, Baldock C, Shuttleworth CA, Kielty CM. 2010. Assembly of fibrillin microfibrils governs extracellular deposition of latent TGF beta. J Cell Sci 123:3006–3018.

Neptune ER, Frischmeyer PA, Arking DE, Myers L, Bunton TE, Gayraud B, Ramirez F, Sakai LY, Dietz HC. 2003. Dysregulation of TGF-β activation contributes to pathogenesis in Marfan syndrome. Nat Genet 33:407–411.

Nistala H, Lee-Arteaga S, Carta L, Cook JR, Smaldone S, Siciliano G, Rifkin AN, Dietz HC, Rifkin DB, Ramirez F. 2010a. Differential effects of alendronate and losartan therapy on osteopenia and aortic aneurysm in mice with severe Marfan syndrome. Hum Mol Genet 19:4790–4798.

Nistala H, Lee-Arteaga S, Smaldone S, Siciliano G, Ramirez F. 2010b. Extracellular microfibrils control osteoblast-supported osteoclastogenesis by restricting TGF{beta} stimulation of RANKL production. J Biol Chem 285:34126–34133.

Nistala H, Lee-Arteaga S, Smaldone S, Siciliano G, Carta L, Ono RN, Sengle G, Arteaga-Solis E, Levasseur R, Ducy P, Sakai LY, Karsenty G, Ramirez F. 2010c. Fibrillin-1 and -2 differentially modulate endogenous TGF-beta and BMP bioavailability during bone formation. J Cell Biol 190:1107–1121.

Ominsky MS, Li X, Asuncion FJ, Barrero M, Warmington KS, Dwyer D, Stolina M, Geng Z, Grisanti M, Tan HL, Corbin T, McCabe J, Simonet WS, Ke HZ, Kostenuik PJ. 2008. RANKL inhibition with osteoprotegerin increases bone strength by improving cortical and trabecular bone architecture in ovariectomized rats. J Bone Miner Res 23:672–682.

Pereira L, Lee SY, Gayraud B, Andrikopoulos K, Shapiro SD, Bunton T, Biery NJ, Dietz HC, Sakai LY, Ramirez F. 1999. Pathogenetic sequence for aneurysm revealed in mice underexpressing fibrillin-1. Proc Natl Acad Sci USA 96:3819–3823.

Ramirez F, Dietz HC. 2009. Extracellular microfibrils in vertebrate development and disease processes. J Biol Chem 284:14677–14681.

Ramirez F, Carta L, Lee-Arteaga S, Liu C, Nistala H, Smaldone S. 2008. Fibrillin-rich microfibrils—Structural and instructive determinants of mammalian development and physiology. Connect Tissue Res 49:1–6.

Rodan GA, Martin TJ. 2000. Therapeutic approaches to bone diseases. Science 289:1508–1514.

Sakai LY, Keene DR, Engvall E. 1986. Fibrillin, a new 350-kD glycoprotein, is a component of extracellular microfibrils. J Cell Biol 103:2499–2509.

Samadfam R, Xia Q, Goltzman D. 2007. Co-treatment of PTH with osteoprotegerin or alendronate increases its anabolic effect on the skeleton of oophorectomized mice. J Bone Miner Res 22:55–63.

Segade F, Suganuma N, Mychaleckhj JC, Mecham RP. 2007. The intracellular form of human MAGP1 elicits a complex and specific transcriptional response. Int J Biochem Cell Biol 39:2303–2313.

Takayanagi H, Iizuka H, Juji T, Nakagawa T, Yamamoto A, Miyazaki T, Koshihara Y, Oda H, Nakamura K, Tanaka S. 2000. Involvement of receptor activator of nuclear factor kappaB ligand/osteoclast differentiation factor in osteoclastogenesis from synoviocytes in rheumatoid arthritis. Arthritis Rheum 43:259–269.

Weinbaum JS, Broekelmann TJ, Pierce RA, Werneck CC, Segade F, Craft CS, Knutsen RH, Mecham RP. 2008. Deficiency in microfibril-associated glycoprotein-1 leads to complex phenotypes in multiple organ systems. J Biol Chem 283:25533–25543.

Werneck CC, Vicente CP, Weinberg JS, Shifren A, Pierce RA, Broekelmann TJ, Tollefsen DM, Mecham RP. 2008. Mice lacking the extracellular matrix protein MAGP1 display delayed thrombotic occlusion following vessel injury. Blood 111:4137–4144.